ICES Journal of Marine Science, 61: 992–1003 (2004)
doi:10.1016/j.icesjms.2004.07.013

Discrete model of fish scale incremental pattern: a formalization of the 2D anisotropic structure

Igor V. Smolyar and Timothy G. Bromage

Smolyar, I. V., and Bromage, T. G. 2004. Discrete model of fish scale incremental pattern: a formalization of the 2D anisotropic structure. – ICES Journal of Marine Science, 61:992–1003.

The structure of growth patterns on fish scales is characteristically anisotropic: the number of circuli and their widths significantly vary with the direction of measurement. We show, however, that because of anisotropy, fish scale growth rate variability can be described in fuzzy terms. The index of structural anisotropy is introduced, which serves as a measure of the fuzziness of growth-rate quantification. A discrete model of fish scale incremental pattern is proposed, which takes into account the incremental structure in 2D. This model is based on a representation of the fish scale pattern as a relay network, taking anisotropy in the form of discontinuities and convergences of incremental structural elements into account, and the widths of growth increments in different directions. The model is used to formalize procedures necessary for the quantification of fish scale growth rate. The capability of the model for analysing objects with similar structural attributes as found in fish scale incremental patterns, such as those found in coral, otoliths, shells, and bones, is demonstrated.

Keywords: boolean function, discrete model, fish scale, fuzziness, graph, growth rate, incremental pattern, index of anisotropy, relay network, structure.

Received 21 July 2003; accepted 8 July 2004.

I. V. Smolyar: SES, Inc. and World Data Center for Oceanography, Silver Spring; Ocean Climate Laboratory, NODC/NOAA, E/OC5, 1315 East West Highway, Room 4308, Silver Spring, MD 20910-3282, USA. T. G. Bromage: Hard Tissue Research Unit, Department of Biomaterials and Biomimetics, New York University College of Dentistry, 345 East 24th Street, New York, NY 10010, USA; tel.: +1 212 998 9597; fax: +1 212 995 4445; e-mail: tim.bromage@nyu.edu. Correspondence to I. Smolyar: tel.: +1 301 713 3290 ext 188; fax: +1 301 713 3303; e-mail: ismolyar@nodc.noaa.gov.

Introduction

Fish scale incremental patterns serve as sources of information, which may help to address broader issues in the marine sciences (Beamish and McFarlane, 1987; Garlander, 1987; Lund and Hansen, 1991). This is so because such patterns, rhythmically constructed from rings called bands, circuli, or growth increments, record events in fish life history and thus, also, the state of the habitat (Matlock *et al.*, 1993; Fabré and Saint-Paul, 1998; Friedland *et al.*, 2000). Fish scale research is hampered, however, because not all steps in their analysis have been formalized (Casselman, 1983). The analytical processing of fish scales has often depended upon qualified and skilled personnel and, in even this case, the results may depend upon an investigator's perceptions and preconceptions (Cook and Guthrie, 1987). The difficulties inherent in formalization procedures and parameterization of fish scales are due to incremental pattern anisotropy, i.e. the size and number of circuli is a function of the direction of measurement (Smolyar *et al.*, 1988; Smolyar *et al.*, 1994). Thus, circuli structure is an important element of the parameterization procedure for studies of fish life history. Presently, there is no method for the quantification of rhythmical structures, which takes anisotropy into account. Our goal is to develop such a method, and to achieve this goal we propose to model the fish scale incremental pattern in order to provide a quantitative description of growth rate variability.

Material

The Atlantic salmon (*Salmo salar*) is an important commercial fish species (Holm *et al.*, 1996), and many works are devoted to the study of its life history via fish scale pattern analyses (MacPhail, 1974). For the purpose of demonstrating the efficacy of the proposed model for understanding life history, it is also acknowledged that the Atlantic salmon scale pattern has a complicated anisotropic structure. Thus, this species was chosen as the exemplar for the present work.

Specimens of fish scales were mounted in water on glass microscope slides and cover slipped. Specimens were imaged with a Leica MZ-APO Stereo Zoom Microscope (Bannockburn, IL) configured with 0.6× planapochromatic lens and substage oblique illumination. Images were transferred to a Leica Quantimet 550 High Resolution Image Analysis System (Cambridge, UK) by an Adimec MX12P 10 bit 1K × 1K grayscale resolution camera (Stoneham, MA) to enhance detail, to improve the visual contrast, and to perform gray level processing protocols resulting in a binary image.

Method

Principal elements

Fish scale patterns are defined by structural elements representing single cycles of development. Such patterns are defined as possessing sequentially formed structural layers over time. Each layer is developed during one cycle of growth. The cycle of growth is described by three variables: (i) a moment at time T when the cycle begins (this temporal instant may be designated arbitrarily as the forming front), (ii) the growth rate at the time T, and (iii) the direction of growth. Graphical elements of the growth cycle are the forming front and the circuli, or band (Figure 1). In the present work we will call this graphical element the incremental band. Because the widths of layers are proportional to growth rate, widths of incremental bands are also a measure of growth rate.

Anisotropy of the fish scale pattern

Consider the commonly used algorithm (Friedland *et al.*, 2000) of the quantification of growth rate for a fish scale pattern (Figure 2). Step 1: transect R has been plotted from its initiation point to its outer margin; Step 2: each incremental band crossed by R has been labeled in the direction of growth. The label of incremental band i is associated with the time T_i. In other words, incremental band i was formed during the time T_i; Step 3: the width of each incremental band is measured and the chart P of incremental bandwidth vs. incremental band number is plotted. Chart P is the quantification of the growth rate along the transect R in terms of the time scale $T = T_1, T_2, \ldots, T_i, \ldots$. However, plotting P is problematical for two reasons due to anisotropy of the fish scale pattern.

First, the shape of chart P is sensitive to the direction of plotting transect R. Minor changes in the direction of plotting the transect R may cause significant changes in P (Figure 2). Thus, P is unstable with respect to the chosen direction of plotting P. Second, the sequence $T = T_1, T_2, \ldots, T_i, \ldots$ describes growth-rate variability along only one transect R. However, fish scale patterns are 2D patterns. When we measure growth rate along one transect we reduce the 2D pattern to a 1D description, and we lose potentially important information relevant to the interpretation of growth rate, which might otherwise be sampled by other transects. Thus, a description of the growth rate of an anisotropic fish scale pattern is a function of its structure.

Parameterization of the growth rate of a fish scale

Consider the construction of a growth rate plot in the case of a fish scale pattern. We draw n transects $R_1, \ldots, R_j, \ldots, R_n$ over the incremental bands in directions perpendicular to the propagating front (Figure 3a). Denote by vertex $a_{i,j}$ the point of intersection of incremental band i with transect R_j (Figure 3b), and the width of the incremental band i at the transect R_j as $w(a_{i,j})$. Growth rate is proportional to increment width, so $w(a_{i,j})$ is a measure of growth rate at time point i along transect R_j (Figure 3c). Consequently, along every transect on the incremental structure, temporal points associated with each increment permit the documentation of growth rate at time points i, i + 1, i + 2,….

If the structure is isotropic, then temporal points may be connected laterally from adjacent transects along T. However, in the case of anisotropy the fish scale pattern may be defined in various ways. Consider an arbitrarily chosen alternative structure only for the incremental band (Figure 4a). Denote by L(T) the number of transects R_j crossing incremental band T, $1 \leq L(T) \leq n$ [L(T) − incremental band length, Figure 4b]. The structure of increment T_i which crosses k lines $R_1, \ldots, R_k$ is determined by the set of k vertices $T_i = (a_{i,1}, a_{i,2}, \ldots, a_{i,k})$.

Because T_i represents the growth rate during the time period i, incremental bands must have the following properties:

(i) Incremental bands cannot intersect;
(ii) Incremental bands cannot merge;
(iii) Incremental band T_i cannot cross R_j more than once. (1)

Thus, any arbitrarily chosen structure of the incremental bands must be in agreement with (1).

Define the width of increment T_i as an average width of $w(a_{i,1}), w(a_{i,2}), \ldots, w(a_{i,k})$:

$$w(T_i) = \left[\sum w(a_{i,j})\right] / L(T_i) \quad (2)$$

We compute values of the parameters L(T) and w(T) for every incremental band T and present the results in a table (Figure 4b). L(T) is a measure of structural integrity or, in other words, the level of continuity expressed by increments for a given number and placement of transects. The greater the value of L(T), the more an increment has been sampled by transects and, thus, the more reason we have to

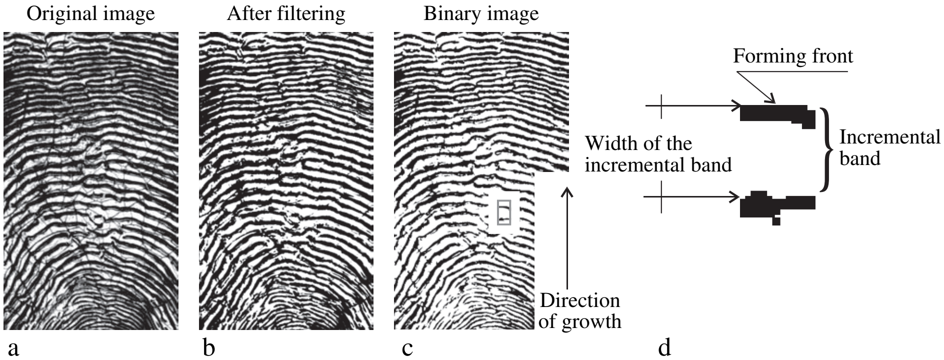

Figure 1. Principal elements of the fish scale pattern. Fish scale patterns are defined by structural elements representing single cycles of development. Images of incremental structures are first acquired (a), then processed with image analytical filters (b), and finally thresholded to produce a binary image (c). On the binary image is defined the incremental band (d). Incremental band T is the part of an incremental structure situated between two adjacent forming fronts.

be confident that w(T) is a measure of the incremental structure and growth rate rather than a source of "noise" caused by increment anisotropy. A lesser value of parameter L(T) reflects more anisotropy and, consequently, we may be less confident in our description of the fish scale pattern (Figure 5a–c).

To describe growth rate of the fish scale pattern we construct a plot "Growth rate vs. Time" (i.e. increment width vs. increment number). This plot should contain as little noise as possible arising from structural anisotropy, or diminishing structural integrity. Thus, to construct the plot we should choose a threshold value of L(T) under which the respective values of w(T) may be interpreted as noise and ignored. However, the current state of knowledge about fish scale pattern formation does not allow us to assume or identify which details might be disregarded as noise, so we should construct a set of plots "w(T) vs. T" for all possible values of L(T). The result is a chart of all 2D plots, rendering a pseudo 3D chart (Figure 5d).

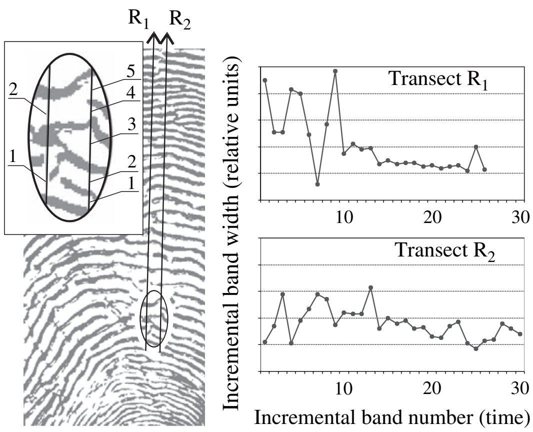

Figure 2. The fish scale pattern as an anisotropic object. Plots of the widths of incremental bands along the time scale $T = T_1, T_2, \ldots$ differ between labeled transects R_1 and R_2 because of anisotropy. This gives us reason to sample the incremental structure with more than one transect.

The 3D chart presents the results for only one arbitrarily chosen structural solution of anisotropic incremental bands (Figure 5c). The portion of the chart where $L(T) = n$ represents the 2D plot "w(T) vs. T" constructed from the set of incremental bands crossed by all transects. That is, it is the portion of the fish scale pattern having maximum (if not ultimate) isotropy and thus relatively high structural integrity. If $L(T) = 1$, then the plot "w(T) vs. T" is constructed from all incremental bands regardless of L(T). That is, it is the portion of the incremental structure having minimum isotropy (i.e. it is most anisotropic) and thus low relative structural integrity. The 2D plots of "w(T) vs. T" constructed of any value between $L(T) = n$ and $L(T) = 1$ may be represented by $L(T) = j$. The goal of the present work is to formalize the procedure for plotting the 3D chart of all 2D plots between and including $L(T) = n$ and $L(T) = 1$ in order to appreciate the growth rate variability of the 2D fish scale pattern. To model the 2D fish scale pattern is a step toward reaching this goal.

Model of the 2D fish scale pattern

Basic concept

The basis for the work presented here is the following:

> The structure of fish scale incremental patterns, together with the widths of incremental bands, are sources of information about the life history of a fish. (3)

From statement (3) it follows that for the parameterization of fish scale incremental pattern it is necessary to formalize the notion of the structure of fish scale patterns. It is desirable that a mathematical presentation of this notion allows one to compare structures.

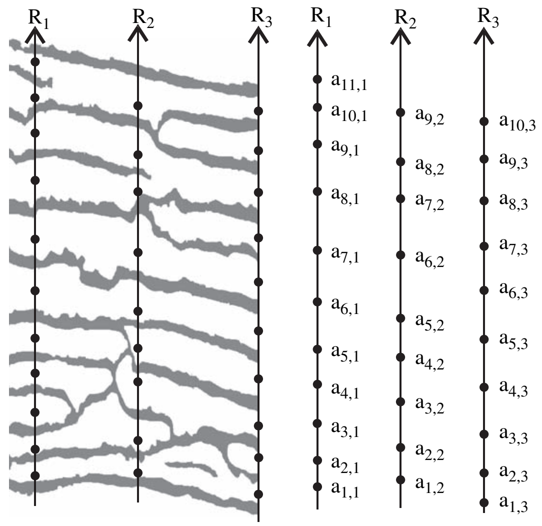

a b

IB-incremental band

IB number	Width of IB		
	R_1	R_2	R_3
1	16	16	21
2	16	25	19
3	24	26	24
4	20	26	29
5	26	28	29
6	31	43	29
7	27	17	23
8	36	29	27
9	21	31	22
10	21		21
11	17		

c

Figure 3. Quantification of the widths of incremental bands for 2D fish scale patterns.

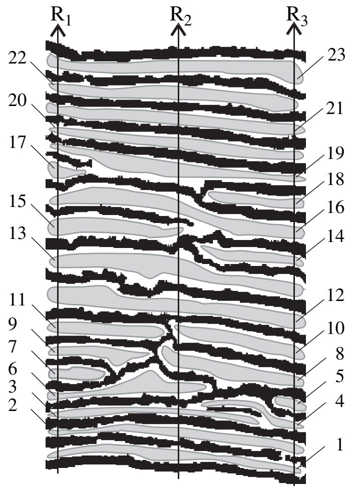

IB-incremental band

IB number	IB width	IB length
1	18	3
2	19	3
3	16	2
4	21	1
5	19	1
6	21	2
7	24	1
8	25	2
9	20	1
10	28	2
11	26	1
12	29	3
13	33	3
14	23	1
15	27	2
16	26	3
17	21	1
18	22	1
19	23	3
20	20	3
21	21	3
22	23	3
23	25	3

a b

Figure 4. Parameterization of the size and structure of the fish scale pattern. The parameter L(T) relates to the actual number of times an incremental band is crossed by a transect. This is a tool for evaluating the level of anisotropy in the incremental structure. In the case of isotropy, L(T) = number of transects for each incremental band. In the opposite case, when L(T) = 1 for each incremental band, the structure is characterized by the highest level of anisotropy.

Size and structure of the fish scale

Results of measured widths of incremental bands along transects R_j, $j = 1, n$ are given in the table $F_{m,n}$ (Figure 3c). Column j of the table contains values $w(a_{1,j})$, $w(a_{2,j})$,….

Represent the incremental band structure as an n-partite graph G(n). Each vertex $a_{i,j}$ of the graph G(n) is associated with the point of intersection between incremental band i and transect R_j (Figure 6a). Vertices $a_{1,j}$, $a_{2,j}$,… situated along the transect R_j, $j = 1, n$ form a class of vertices A_j. Vertices belonging to the class A_j, $j = 2, n - 1$, may only be connected across to vertices from classes A_{j-1} and A_{j+1}. The vertex $a_{i,j}$ is connected with the vertex $a_{i,j+1}$ if edge $a_{i,j}$ $a_{i,j+1}$ crosses no forming fronts. Figure 6 depicts typical elements of the incremental structure (Figure 6b) and their corresponding graphs (Figure 6a).

The extent to which the model $M = \{G(n), F_{m,n}\}$ of the fish scale pattern is representative of the initial image depends upon the number (i.e. sampling density) of transects R_j. It follows that with few transects, little processed image detail will be sampled in consideration of the model of the incremental structure. At $n \to \infty$ the model $M = \{G(n), F_{m,n}\}$ will be the complete representation of the processed image.

The fish scale pattern as a relay network and the index of structural anisotropy

A constructed relay network of a fish scale pattern allows one to quantify the contribution of each discontinuity and convergence to the variability of the growth rate. This information is necessary to establish a correspondence between the structure of a fish scale pattern and events in the life of the fish.

Denote the plot of growth rate for a whole incremental structure in the 3D space illustrated by "Incremental bandwidth vs. Incremental band number vs. Structural integrity" by GR (Figure 5d). This chart represents

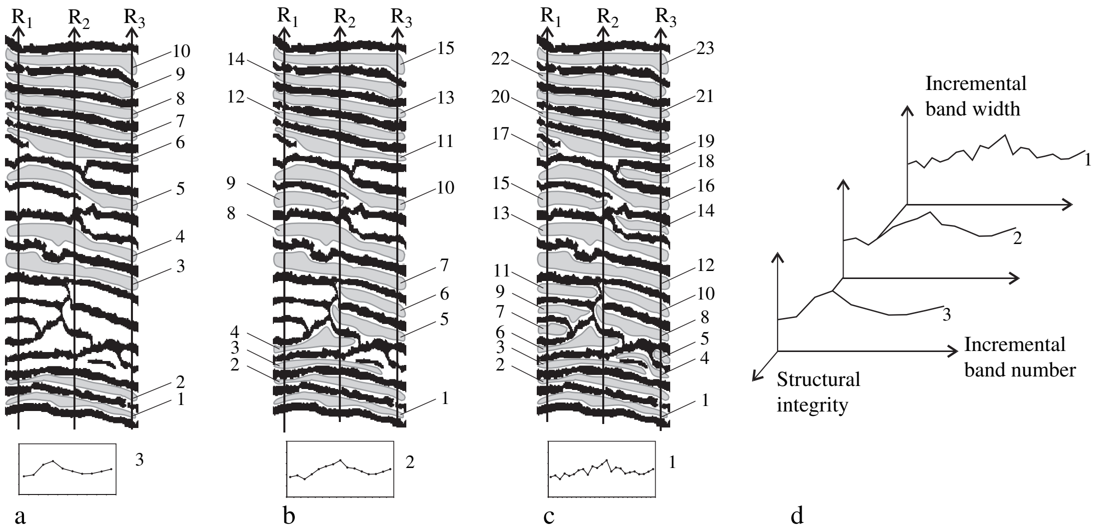

Figure 5. A 3D representation of growth rate of the fish scale pattern containing anisotropy. Incremental bands crossed by at least one (a), two (b), or all three (c) transects are measured, charted, and compiled into a 3D chart (d).

incremental growth rate variability for only one possible version of its structure (i.e. increment discontinuities have been reconstructed in only one of all possible paths). How may we propose an algorithm that allows one to choose an appropriate version of incremental bands structure? Consider two different approaches to construct this algorithm.

The first approach is to choose the optimal incremental band structure in the course of plotting GR. To do this we must define the criterion K by which we determine the optimal variant of the incremental bands structure. The solution involves a search for the variant that satisfies the properties given in (1) and which provides an extreme value of K. Though all fish scale patterns contain forming fronts, specific morphologies may vary. As a result, the choice of parameters that one may use to define criterion K will depend upon one's objects of study. The present work does not propose to choose any particular value of K for different fish scale patterns. However, if K is neglected, a description of different patterns of incremental bands in the form of an n-partite graph G(n) permits one to state the problem as follows: We should find the set of paths in G(n) connecting vertices of classes $A_1, \ldots, A_n$, which includes all vertices of the graph that satisfy (1). This problem statement is a sort that is typical in graph theory, and a wide range of methods have been developed for their solution (Harrary, 1973).

Consider an alternative approach to the definition of incremental band structure than one based on calculating K. To understand how anisotropy can affect the shape of GR we would have to compare GR plotted for all possible versions of the incremental structure. However, due to numerous discontinuities and convergences, a phenomenal

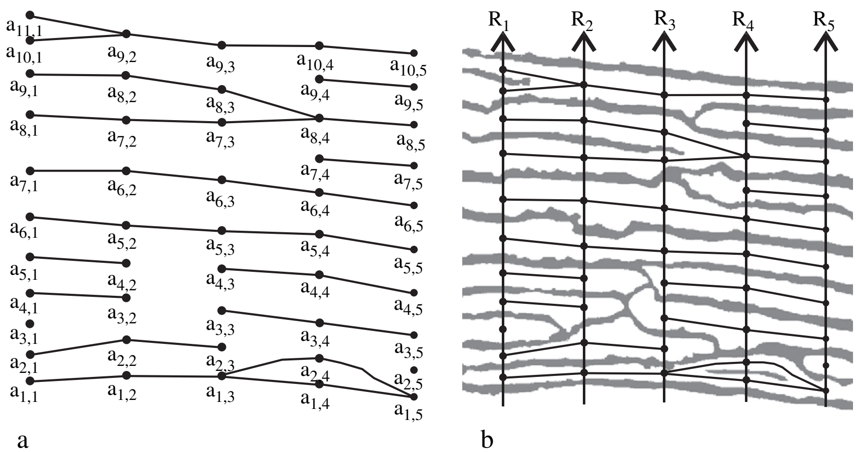

Figure 6. Quantification of the anisotropic structure of the fish scale pattern.

number of possible versions may be found in only a small portion of many fish scale patterns (Figure 1).

Our solution to this predicament is to select computationally the two versions V_i and V_j that differ maximally from one another in their incremental band structure, and to plot the $GR(V_i)$ and $GR(V_j)$ for both versions V_i and V_j. If $GR(V_i)$ and $GR(V_j)$ do not considerably differ, then there is no reason to test for all possible versions of the incremental structure. To apply this solution we must provide answers to the following questions: (i) how may we quantify the difference between versions of incremental structure, and (ii) how to create versions V_i and V_j that differ maximally from one another in their structure?

To answer these questions, examine a simple fragment of a fish scale pattern (Figure 7a). The combination of two incremental bands T_1 and T_2 form two versions, V_1 and V_2, of the incremental bands structure (Figure 7a). To define all possible versions, introduce the notion of "door open" and "door closed" (Figure 7b). Figure 7c represents all possible versions of the states of doors X and Y and all possible versions of the incremental bands structure. Thus, "states of doors" are responsible for the incremental bands structure. Because X takes two values, we used the Hamming metric (Hamming, 1971) to quantify the difference $D(V_i, V_k)$ between versions of the incremental structures V_i and V_k:

$$D(V_i, V_k) = |X_i - X_k| + |Y_i - Y_k| + \ldots,$$

where X_k and X_i are the state of door X for versions of incremental band structures V_k and V_i, respectively. For versions of incremental band structures V_1 and V_2 illustrated in Figure 7a, the difference between V_1 and V_2 is $D(V_1, V_2) = |0 - 1| + |1 - 0| = 2$. This is the maximum possible difference between versions of the structure for the fragment portrayed in Figure 7a. The procedure for generating versions V_i and V_j that differ maximally from one another is the following: (i) define V_1 by randomly choosing the states of all doors, (ii) define V_2 by changing the state of all doors, which are responsible for V_1, and (iii) plot charts $GR(V_1)$ and $GR(V_2)$ for both versions of incremental band structures V_1 and V_2.

Denote the distance between $GR(V_i)$ and $GR(V_j)$ surfaces by $D_a(GR(V_i), GR(V_j))$. The $D_a(GR(V_i), GR(V_j))$ value cannot exceed $w_{max}(T) - w_{min}(T)$, where $w_{max}(T)$ and $w_{min}(T)$ are the widest and the narrowest incremental bands, respectively. The distance $D(GR(V_i), GR(V_j))$ between $GR(V_i)$ and $GR(V_j)$ is conveniently represented in a continuous scale [0,1]. If $D = 1$, the distance between $GR(V_i)$ and $GR(V_j)$ surfaces is maximal and, in this situation, a description of growth rate variability greatly depends on incremental band structure. If $D = 0$, this points to the fact that incremental structure growth rate is independent of incremental band structure, i.e. the incremental structure is isotropic. Values $0 < D < 1$ take an intermediate place between the two extreme cases. Let us denote $D(GR(V_p), GR(V_q))$ by:

$$D(GR(V_i), GR(V_j)) = D_a(GR(V_i), GR(V_j)) / (w_{max}(T) - w_{min}(T)) \quad (4)$$

Parameter (4) calculates the sensitivity of the GR to variability in the incremental band structure. This parameter will be named the index of structural anisotropy of the fish scale pattern.

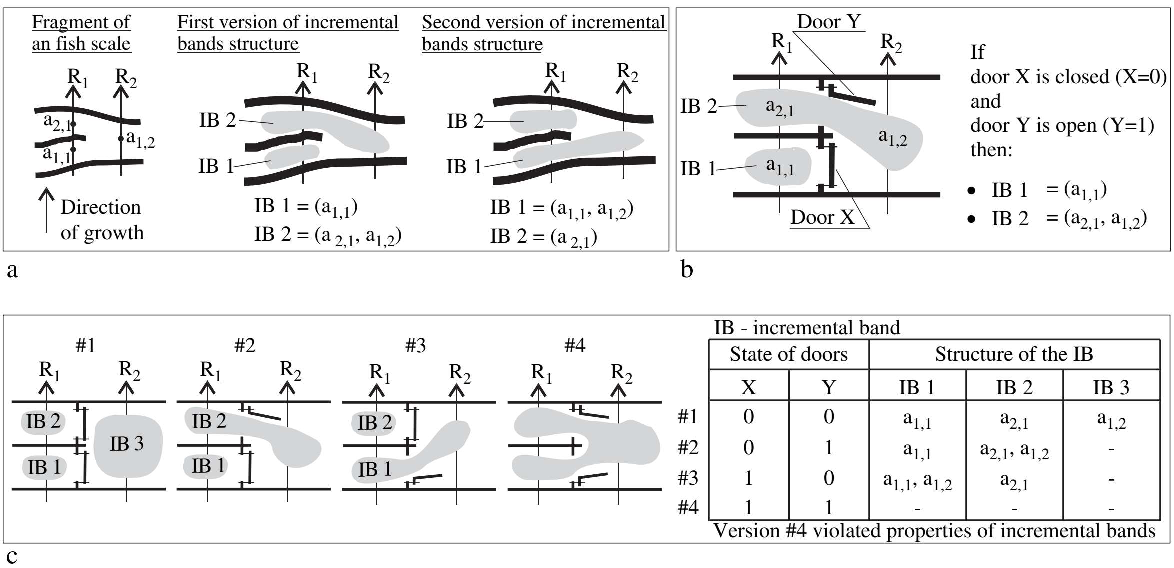

Figure 7. Structure of the fish scale pattern as a relay network. Different versions of the incremental band structure are represented in (a). The structure of the incremental band is a function of the state of the "door" (b). A description of all versions of the incremental band structure is shown in (c).

From the image to the model of the fish scale pattern

Consider the algorithm required to construct the model $M = \{G(n), F_{m,n}\}$. Our research protocol presently begins with the acquisition of a digital grayscale image in raster format (Figure 1). In the first step, filters are applied to render a binary black and white image (i.e. grayscale levels 0 and 255 only) (Figure 8a). The image processing decisions made in this step are based upon the specific objects of study and one's understanding of the incremental structure. Transects are then plotted manually to obtain what may be judged to provide the correct direction of growth and, thus, improved accuracy in the quantification of growth rate variability. The binary image is then automatically converted into vector format. This allows one to define coordinate points of intersections of transects R_j, $j = 1, n$ with forming fronts, permitting one to make measurements of incremental bandwidths along transects $R_1, \ldots, R_n$. The result of these operations in the first step is a table $F_{m,n}$ which describes the widths of incremental bands along transects $R_1, \ldots, R_n$.

As the second step, the binary image is inverted. Incremental bands, now black, are automatically converted into vector format and rendered as a line connecting vertices $a_{i,j}$ and $a_{i,j+1}$ (Figure 8b). This procedure allows one to assign a label to each vertex $a_{i,j}$ and to determine the possibility of the connection of two vertices $a_{i,j}$ and $a_{i,j+1}$ with a line crossing no forming fronts. Thus, the matrix of connections of class A_j vertices with those from class A_{j+1} is constructed. The distance between two nearby points on transect R_j is the width of the incremental band $a_{i,j}$. These two steps result in a model $M = \{G(n), F_{m,n}\}$ of the fish scale pattern.

Assumptions and limitations

The proposed approach to the description of growth-rate variability of anisotropic fish scale patterns is based on assumption and limitations. These are:

(i) Assumption: width of the incremental band T_i, measured along different transects is unimodally distributed;
(ii) Limitation 1: cannot distinguish artifact from incremental structure;
(iii) Limitation 2: mathematical comparison of two independent structures of fish scale patterns remains unresolved.

The assumption permits one to use Equation (2) to calculate the average width of the incremental band T_i. If this assumption is not valid (e.g. a bimodal distribution of increment widths), then the notion of growth rate variability of a whole 2D incremental structure makes no sense.

With respect to limitation 1, it will be hard to distinguish patterns from incremental structure without specific pattern recognition algorithms designed for each unique object of study. The method proposed here averages incremental width, or growth rate, along the entire course of the sampling area. Limitation 2 obviates our ability to quantitatively compare structures of two fish scale patterns. For now, the method only allows us to make qualitative comparisons of different versions of the incremental band structure of a fish scale pattern.

Discussion

Fish scale pattern anisotropy results in less than perfect descriptions of growth rate of 2D fish scale patterns, and thus growth-rate variability may only be described in "fuzzy" terms. The index of structural anisotropy is a measure of this fuzziness, providing us with some perspective on the confidence we may have in the measurements. Use the problem of stock identification (Cook and Guthrie, 1987) to illustrate how the model of the fish scale pattern could contribute to the solution of this problem. The algorithm of stock identification consists of three main steps.

Step 1: measurements of the widths of incremental bands are performed along an arbitrarily chosen transect R and the 2D chart "Incremental bandwidth vs. Incremental band number" is plotted. The model $M = \{G(n), F_{m,n}\}$ actually permits the use of multiple transects and the plotting of 2D charts with different values of structural integrity L(T); one of these charts (Figure 5) could be used for Step 2 (below). The shape of the chart "Incremental bandwidth vs. Incremental band number" depends on two variables: the number of transects and L(T). If one chose few transects, then L(T) will be low with a consequent loss of useful information about the growth rate variability. In the opposite case, the risk of noise on 2D chart is increased. A compromise between the number of transects and the value of L(T) may be found by experimentation and depends upon the fish scale structure of the individual species of fish investigated.

Step 2: fish scale pattern is described in terms of features $x_1, x_2, \ldots$, these features having been derived from the 2D chart. The model $M = \{G(n), F_{m,n}\}$ permits the use of the index of structural anisotropy as the new feature of summer/winter growth zones.

Consider the results of the incremental processing of an Atlantic salmon fish scale (Figure 9). Charts $GR(V_1)$ and $GR(V_2)$ reflect two periods of growth of the scale ΔT_1 and ΔT_2. The first period ΔT_1 is characterized by the high growth rate, and the second ΔT_2 by the low growth rate. Surface 3 is the mathematical subtraction (i.e. comparison) of $GR(V_1)$ from $GR(V_2)$, demonstrating that anisotropy is confined mainly to the growth period ΔT_1. The visual comparison of charts describing anisotropy for two fish scales derived from two different fish also demonstrates that

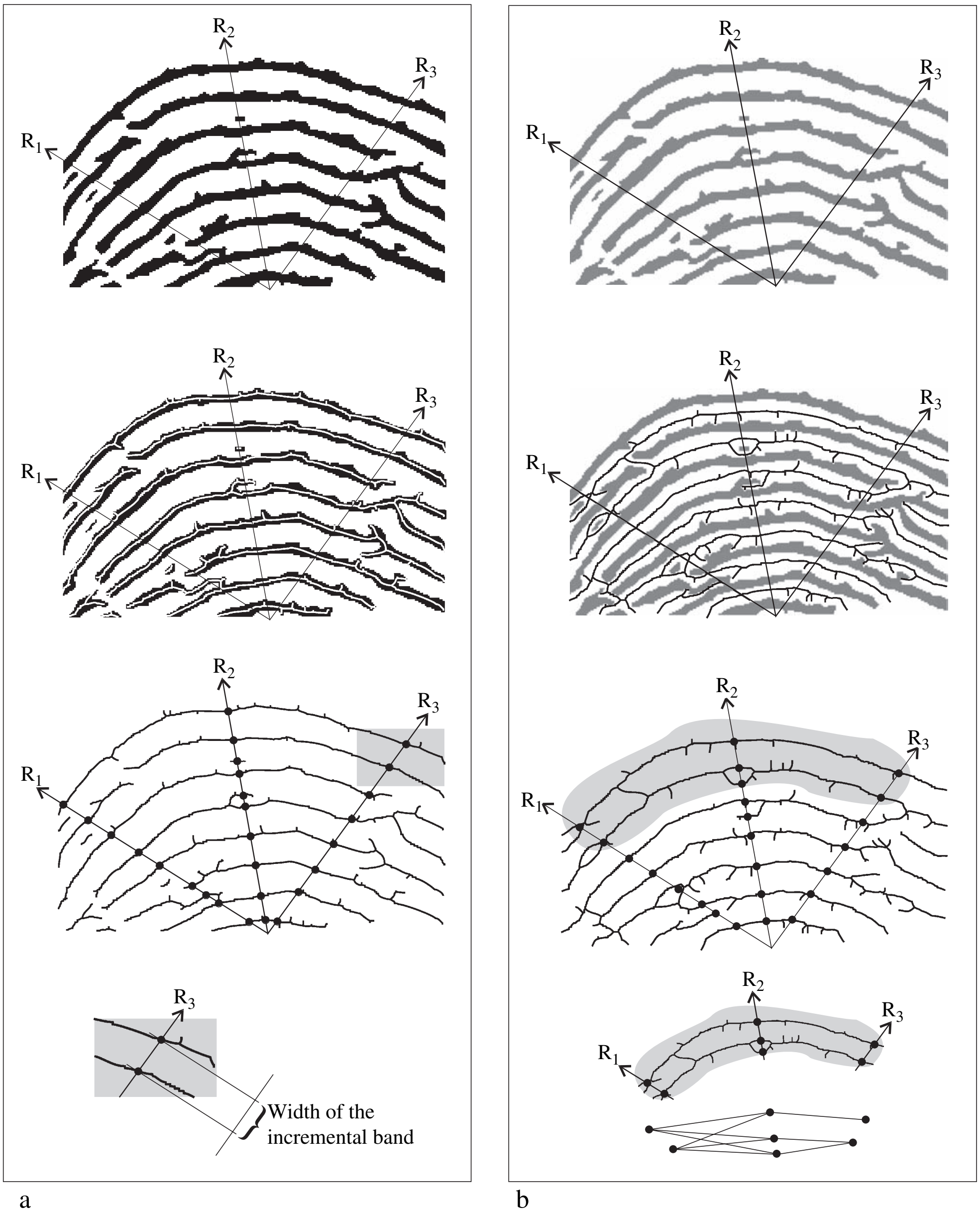

Figure 8. From the image to the model of the fish scale pattern. Vectorization of the forming fronts allows one to extract structural detail for defining the widths of incremental bands (a), and vectorization of the incremental bands is required for defining the incremental structure (b).

anisotropy is higher during the growth period ΔT_1 than during the growth period ΔT_2 (Figure 10). The index of structural anisotropy of fish scale 1 is less than that of fish scale 2 (Figure 10).

Step 3: mathematical methods are used to quantify the differences between growth rates of fish scales of various fish stocks for the purpose of relating a fish of unknown origin to one of known stock. The model $M = \{G(n), F_{m,n}\}$ permits the use of the index of structural anisotropy derived from the whole scale as a measure of the fuzziness of growth rate quantification. Thus, the index of structural anisotropy of fish scales used for stock identification could serve as the source of information about the accuracy of the 2D chart "Incremental bandwidth vs. Incremental band number". A high value of the index of structural anisotropy may lead to an error in stock identification. Thus, the index of structural anisotropy allows one to understand the influence of fuzziness on the accuracy of the findings.

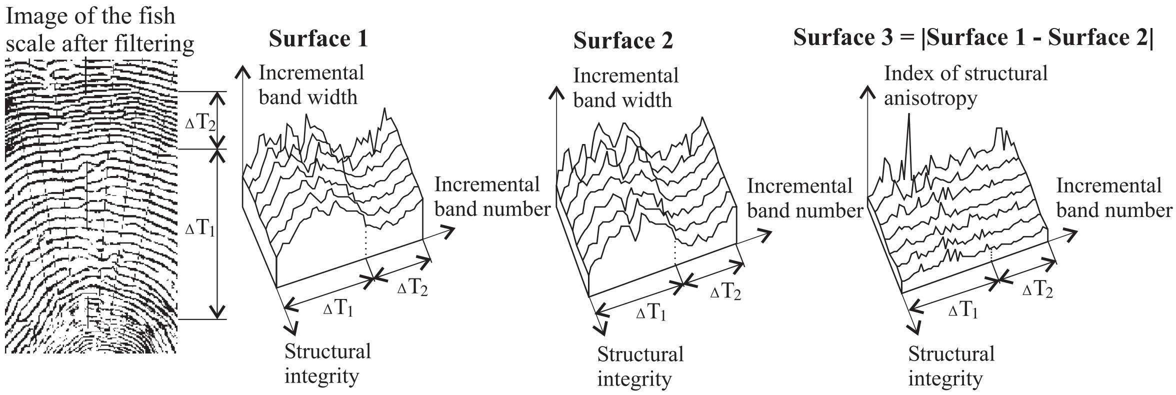

Figure 9. Index of structural anisotropy of images of fish scales. Surface 1 is the variability of the growth rate of the fish scale for one version of the incremental band structure $GR(V_1)$. Surface 2 is the variability of the growth rate of the fish scale for a second version of the incremental band structure $GR(V_2)$. $V_1 - V_2 =$ maxima. Surface 3 is equal to Surface 1 minus Surface 2, which is a measure of anisotropy of the fish scale.

Capability of the model. Areas of potential application

Fish scales and environmental database development

Fish scale incremental patterns possess a unique combination of features: Fish scales are easily available, their preparation for image processing is very simple, and ichthyologists have used fish scale patterns for decades as a source of information about the life history of fish as well as the state of the environment (Pepin, 1991; Friedland, 1998). Because of these features, many marine institutions around the world have maintained collections of fish scales of various species of fish from the World Ocean for decades. A database of results obtained from incremental studies, together with the oceanographic database of the World Ocean (Levitus *et al.*, 1998), can provide new tools for studying the biological resources, climate variability, and conservation of ocean life. However, only a small portion of these collections has employed incremental analysis due to the lack of a formal model such as that proposed here.

The model $M = \{G(n), F_{m,n}\}$ of the fish scale pattern allows us to develop a database of hundreds of thousands of fish scales. The principal steps of the fish scale pattern processing protocol are formalized and may be automated, thus excluding time and labor intensive manual processing.

The only element of the processing procedure not considered automatic in the present work is the operation of plotting transects $R_1, \ldots, R_n$. Knowledgeable practitioners must presently define this operation for each category of incremental structure. Until such time that automatic procedures exist, one can increase the number of transects in order to account for as much incremental detail as necessary for any specific problem.

Incremental patterns in nature

We have described fish scales as belonging to the class of objects we refer to as incremental patterns. Let us consider other examples of incremental patterns.

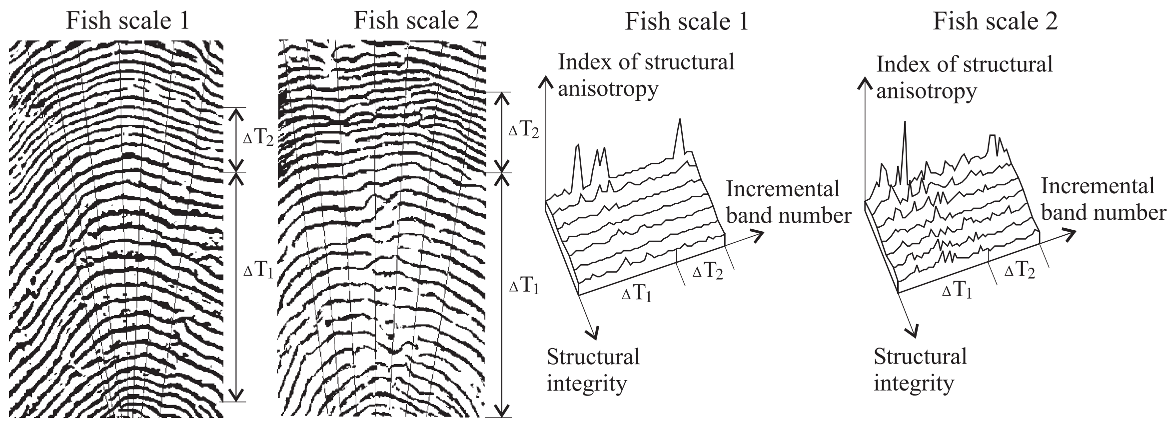

Figure 10. Index of structural anisotropy for scales from two different fish.

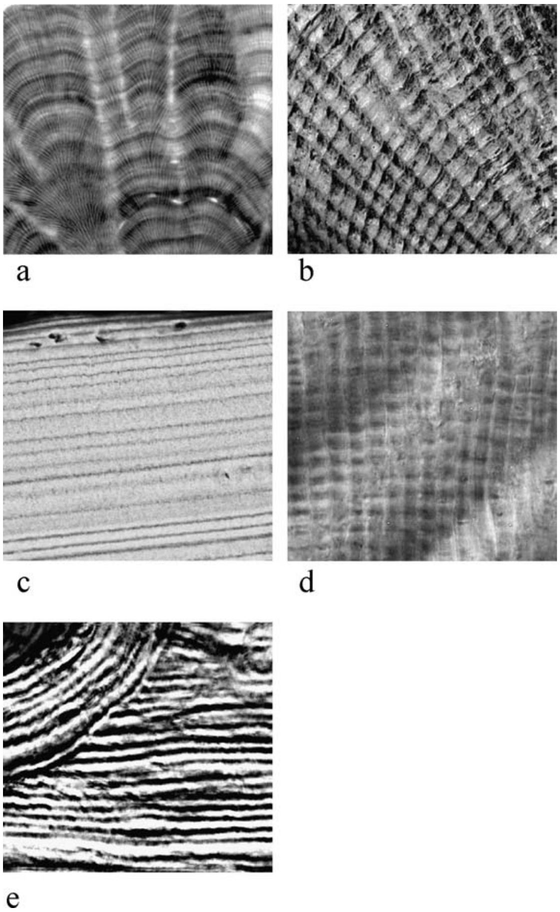

Figure 11. Examples of incremental patterns. (a) Coral. This is an x-radiographic positive of a 7-mm-thick slice of the coral *Porites lobata*, Great Barrier Reef, Australia. Image courtesy of Dave Barnes, Australian Institute of Marine Science. (b) Bivalve shell. Shell of *Codakia orbicularis* (900–1500 AD archeological site of Tanki Flip Henriquez, Aruba) observed with oblique light on a Leica MZ-APO Stereo Zoom Microscope and acquired with Syncroscopy™ Montage Explorer. Specimen courtesy of Marlene Linville, Graduate School of the City University of New York, and the Archeological Museum of Aruba under the direction of Arminda Ruiz. Field width = 13.7 mm. (c) Fish otolith. Otolith of North Atlantic cod (*Gadus morhua*) collected at Langenes, Norway, was observed with a LEO S440 Scanning Electron Microscope operated in backscattered electron imaging mode. Specimen courtesy of Sophia Perdikaris, Brooklyn College, CUNY. (d) Dental hard tissues. Human enamel (Medieval archeological sample from Tirup, Denmark) observed with circularly polarized light with a Leica DMRX/E Universal Microscope and acquired with Syncroscopy™ Montage Explorer. Image illustrates daily (horizontal) and near-weekly (lower left to upper right) increments. Image courtesy of Rebecca Ferrell, Pennsylvania State University. Specimen courtesy of Jesper Boldsen, Anthropological Database, University of Southern Denmark. Field width = 130 μm. (e)Bone image of lamella (horizontal) increments derives from a 100-μm-thick section from the mid-shaft femur of a 28-year-old female, observed with circularly polarized light on a Leica DMRX/E Universal Microscope. Note remodeling event at upper left, representing a different time and spatial organization of bone tissue. Image courtesy of Haviva Goldman, Hahnemann School of Medicine. Specimen derived from the Victorian Institute of Forensic Medicine, courtesy of John Clement, University of Melbourne. Field width = 350 μm.

The widths of annual growth bands in coral (Figure 11a), referred to as "density bands" in x-radiographic studies of coral slabs, are proportional to the growth rate (Knutson and Smith, 1972; Barnes and Lough, 1993). Coral banding patterns have, for instance, been related to El Niño climate variability (Urban *et al.*, 2000) and Milankovitch orbital forcing chronologies in the distant past (Stirling *et al.*, 2001).

Growth lines in molluscan shells (Figure 11b) are represented externally and internally (Pannella and MacClintock, 1968; Clark, 1974). Macroscopically, annual growth lines are often prominent surface features between which lunar or solar month, fortnightly tidal, or daily features may be observed. These growth lines are also observed internally in histological section. Some taxa form sub-daily growth lines thought to relate to activity levels (Gordon and Carriker, 1978). Shell age and condition of the marine environment are estimated by variation in the widths of growth lines.

Daily growth increments are observed in fish otolith cross-sections (Figure 11c), the measurements of which are commonly used for age and growth rate variability studies in wild (e.g. Bolz and Lough, 1988; Kingsmill, 1993; Linkowski *et al.*, 1993) and reared environments where variables, such as temperature and salinity, may be altered in order to assess their effects on growth (e.g. Ahrenholz *et al.*, 2000). In addition to daily increments, it has been observed that seasonal changes in increment widths reveal annular band structures (Clear *et al.*, 2000). Anomalously narrow annular bands have been linked to El Niño events (Woodbury, 1999).

Dental hard tissues (Figure 11d) are composed of incremental structures representing several time scales. Enamel and dentine both contain daily (circadian) and near-weekly (circaseptan) rhythms (e.g. Boyde, 1964; Bromage and Dean, 1985; Bromage, 1991), while cementum harbors an annual seasonal rhythm (e.g. Klevezal, 1996; Klevezal and Shishlina, 2001).

Bone (Figure 11e) is rarely considered as an incremental structure, yet like dental hard tissues, there is an incremental structure called the lamella. In one study of growing rats flown aboard the NASA Space Shuttle, the widths of lamellae have been interpreted as proportional to bone growth rate (Bromage *et al.*, 1997, 1998). In that study, it could be confirmed that one lamella related to one day's growth.

The fundamental similarities between fish scale incremental patterns and other such patterns from diverse biological samples are as follows:

(i) Incremental bands of different incremental patterns represent one cycle of the object growth. The width of the incremental band is a measure of the growth rate of the incremental pattern.
(ii) Growth rates of incremental patterns are a function of internal and external factors. Thus, the life history of incremental patterns may be recognized via analyses of growth-rate variability. This is also true for fish scales.
(iii) Incremental bands of different incremental structures, including fish scales, have numerous breaks and confluences, which lead to structural anisotropy of incremental patterns.
(iv) The structure of incremental bands is the source of diagnostic information about events in the life history of incremental patterns.

Incremental patterns (Figure 11a—e) are thus potentially a primary source of information about the duration and amplitude of periodic phenomena as well as about other natural history events occurring during formation. Information about cyclicity, interactions between cycles, and perturbations to the responding system are all inherently contained within incremental patterns. Further, because many incremental structures preserve their pattern, and thus information about growth rate well after formation, their analysis provides a means of appreciating aspects of organismal life history or accretion rates in the recent and distant past that could not be examined otherwise.

Conclusion

A key element of the present work is the notion of fish scale incremental pattern structure. Such structures manifest themselves as visual signals that provide information about the history of pattern formation (Ball, 1999; Ben-Jacob and Levine, 2000). To decode these signals is important from both a theoretical and a practical point of view. The parallel drawn between a relay network (e.g. an electrical circuit) and fish scale pattern structure permits one to use the relay network as a tool for modelling fish scale growth rate variability as a function of changes in its structure.

Acknowledgements

Galina A. Klevezal and Phillip V. Tobias provided seminal commentary on the manuscript, for which we are extremely grateful. The cooperation with the Murmansk Marine Biological Institute (Russia), and particularly Aleksandr Chernitsky, Gennady Matishov, and Aleksey Zuyev made this work possible. We very much appreciate Bernice Kurchin, AMICA Friend, for her support of the Analytical Microscopy and Imaging Center in Anthropology, Hunter College, where this work was performed. The work presented here was generously supported by grants from the National Aeronautics and Space Administration (NAG5-6806) and the National Science Foundation (BCS-0079700).

References

Ahrenholz, D. W., Squires, D. D., and Rice, J. A. 2000. Periodicity of increment formation in otoliths of overwintering postlarval and prejuvenile Atlantic menhaden, *Brevoortia tyrannus*. Fishery Bulletin, 98: 421—426.

Ball, P. 1999. The Self-Made Tapestry. Oxford University Press, Oxford. 287 pp.

Barnes, D. J., and Lough, J. M. 1993. On the nature and causes of density banding in massive coral skeletons. Journal of Experimental Marine Biology and Ecology, 167: 91—108.

Beamish, R. J., and McFarlane, G. A. 1987. Current trends in Age Determination Methodology. *In* Age and Growth of Fish, pp. 15—42. Ed. by R. C. Summerfelt, and G. E. Hall. Iowa State University, Ames, Iowa. 544 pp.

Ben-Jacob, E., and Levine, H. 2000. The artistry of nature. Nature, 409: 985—986.

Bolz, G. R., and Lough, R. G. 1988. Growth through the first six months of Atlantic cod, *Gadus morhua*, and haddock, *Melanogrammus aeglefinus*, based on daily otolith increments. Fishery Bulletin, 86: 223—235.

Boyde, A. 1964. Estimation of age at death of a young human skeletal remains from incremental lines in the dental enamel. Excerpta medica International Congress Series 80: 36. Proceedings of the 3rd International Meeting Forensic Immunology Medicine Pathology and Toxicology. London.

Bromage, T. G. 1991. Enamel incremental periodicity in the pigtailed macaque: a polychrome fluorescent labeling study of dental hard tissues. American Journal of Physical Anthropology, 86: 205—214.

Bromage, T. G., and Dean, M. C. 1985. Re-evaluation of the age at death of immature fossil hominids. Nature, 317: 525—527.

Bromage, T. G., Smolyar, I., Doty, S. B., Holton, E., and Blayvas, A. 1997. Quantitation of growth-rate variability in mineralized tissue incremental structures. American Journal of Physical Anthropology(Suppl. 24): 83.

Bromage, T. G., Smolyar, I. V., Doty, S. B., Holton, E., and Zuyev, A. N. 1998. Bone growth rate and relative mineralization density during space flight. Scanning, 20: 238—239.

Casselman, J. M. 1983. Age and growth assessment of fish from their calcified structures — techniques and tools. *In* OAA Technical Report NMFS 8. Proceedings of the International Workshop on Age Determination of Oceanic Pelagic Fishes: Tunas, Billfishes, and Shark, pp. 1—17. Ed. by E. D. Prince, and L. M. Pulos. 212 pp.

Clark II, G. 1974. Growth lines in invertebrate skeletons. Annual Review of Earth and Planetary Sciences, 2: 77—99.

Clear, N. P., Gunn, J. S., and Rees, A. J. 2000. Direct validation of annual increments in the otoliths of juvenile southern bluefin tuna, *Thunnus maccoyii*, by means of a large-scale mark—recapture experiment with strontium chloride. Fishery Bulletin, 98: 25—40.

Cook, R. C., and Guthrie, I. 1987. In-seasonal stock identification of sockeye salmon (*Oncorhynchus nerka*) using scale pattern recognition. *In* Sockeye Salmon (*Oncorhynchus nerka*) Population Biology and Future Management, pp. 327—334.

Ed. by H. D. Smith, L. Margolis, and C. C. Wood. Canadian Special Publication of Fisheries and Aquatic Sciences 98. 486 pp.

Fabré, N. N., and Saint-Paul, U. 1998. Annulus formation on scales and seasonal growth of the Central Amazonian anostomid *Schizodon fasciatus*. Journal of Fish Biology, 53: 1–11.

Friedland, K. D. 1998. Ocean climate influences on critical Atlantic salmon (*Salmo salar*) life history events. Canadian Journal of Fisheries and Aquatic Sciences, 55(Suppl. 1): 119–130.

Friedland, K. D., Hansen, L. P., Dunkley, D. A., and MacLean, J. C. 2000. Linkage between ocean climate, post-smolt growth, and survival of Atlantic salmon (*Salmo salar* L.) in the North Sea area. ICES Journal of Marine Science, 57: 419–429.

Garlander, K. D. 1987. A history of scale age and growth studies of North American freshwater fish. *In* Age and Growth of Fish, pp. 3–14. Ed. by R. C. Summerfelt, and G. E. Hall. Iowa State University, Ames, Iowa. 544 pp.

Gordon, J., and Carriker, M. R. 1978. Growth lines in a bivalve mollusk: Subdaily patterns and dissolution of the shell. Science, 202: 519–520.

Hamming, R. W. 1971. Introduction to Applied Numerical Analysis. McGraw Hill, New York. 331 pp.

Harrary, F. 1973. Graph Theory. Mir, Moscow. 300 pp.

Holm, M., Holst, J., and Hansen, L. 1996. Atlantic salmon survey in the Norwegian Sea from July 1991–August 1995. Aquaculture, 1996(1): 21.

Kingsmill, S. 1993. Ear stone speak volumes to fish researchers. Science, 260: 1233–1234.

Klevezal, G. A. 1996. Recording Structures of Mammals: Determination of Age and Reconstruction of Life History. A.A. Balkema, Rotterdam. 244 pp.

Klevezal, G. A., and Shishlina, N. I. 2001. Assessment of the season of death of ancient human from cementum annual layers. Journal of Archaeological Science, 28: 481–486.

Knutson, D. W., and Smith, S. V. 1972. Coral chronometers: seasonal growth bands in reef corals. Science, 177: 270–272.

Levitus, S., Boyer, T., Conkright, M., O'Brien, T., Antonov, J., Stephens, C., Stathoplos, S., Johnson, D., and Gelfeld, R. 1998. NOAA Atlas NESDIS 18, World Ocean Database 1998: Volume 1: Introduction. U.S. Government Printing Office, Washington, D.C. 346 pp.

Linkowski, T. B., Radtke, R. L., and Lenz, P. H. 1993. Otolith microstructure, age and growth of two species of *Ceratoscopelus* (Osteichthyes: Myctophidae) from the eastern North Atlantic. Journal of Experimental Marine Biology and Ecology, 167: 237–260.

Lund, R. A., and Hansen, L. 1991. Identification of wild and reared Atlantic salmon, *Salmo salar* L. using scale characters. Aquaculture and Fisheries Management, 22: 499–508.

MacPhail, D. K. 1974. Photographic reproductions of Atlantic salmon scales from fish of known sea ages. Technical Report Series No. MAR T-74-1. Resource Development Branch. Maritimes Region. Fisheries and Marine Service. Environment Canada. 55 pp.

Matlock, G. C., Colura, R. L., and McEachron, L. W. 1993. Direct validation of black drum (*Pogonias cromis*) ages determined from scales. Fishery Bulletin, 91: 558–563.

Pannella, G., and MacClintock, C. 1968. Biological and environmental rhythms reflected in molluscan shell growth. Journal of Paleontology, 42: 64–80.

Pepin, P. 1991. The effect of temperature and size on development, mortality and survival rates of the pelagic early life stages of marine fishes. Canadian Journal of Fisheries and Aquatic Sciences, 48: 503–518.

Smolyar, I. V., Almeida, F., and Barnett J. 1994. The anisotropic structure of fish scales patterns and its consideration in the quantification of seasonal growth. *In* Program and Abstracts: Flatfish Biology Workshop, Mystic, Connecticut, 26–27.

Smolyar, I. V., Ermolaeva, I., and Chernitsky, A. 1988. Mathematical Model of Fish Scales and Algorithms for their Analysis. Kola Branch of the Russian Academy of Sciences, Apatity. 22 pp.

Stirling, C. H., Esat, T. M., Lambeck, K., McCulloch, M. T., Blake, S. G., Lee, D.-C., and Halliday, A. N. 2001. Orbital forcing of the marine isotope stage 9 interglacial. Science, 291: 290–293.

Urban, F. E., Cole, J. E., and Overpeck, T. 2000. Influence of mean climate change on climate variability from a 155-year tropical Pacific coral record. Nature, 407: 989–993.

Woodbury, D. 1999. Reduction of growth in otoliths of widow and yellowtail rockfish (*Sebastes entomelas* and *S. flavidus*) during the 1983 El Niño. Fishery Bulletin, 97: 680–689.